Solar-driven CO₂ Methanation Over Nickel-based Catalysts for Solar Fuel Production: An Experimental and Mechanism Study

Fan Sun[1,2], Xueli Xing[2,3], Yu Xin[2,3], Hui Hong[2,3,*]

1 International Research Center for Renewable Energy & State Key Laboratory of Multiphase Flow in Power Engineering, Xi'an Jiaotong University, Xi'an, 710049, China.

2 Institute of Engineering Thermophysics, Chinese Academy of Sciences, Beijing 100190, China.
3 University of Chinese Academy of Sciences, Beijing 100049, China.
(*Corresponding Author: huihong@iet.cn)

ABSTRACT

The CO₂ methanation (that is, Sabatier reaction), has been considered as a promising way to recycle and utilize CO₂. However, the industrial Sabatier process is energy intensive and traditionally powered by fossil fuels. Harvesting solar energy for the conversion of CO₂ into solar fuels offers a sustainable and green solution to alleviating energy and environmental issues. In this work, solar-driven CO₂ methanation over nickel-based catalysts was investigated under concentrated solar irradiation. A CO₂ conversion rate of approximately 87%, with 100% selectivity towards CH₄ and a reaction rate of 380 mmol/g_{Ni}/h were achieved under concentrated UV-visible-IR irradiation at 350 °C on 15 wt% Ni/Al₂O₃. The temperature required to achieve maximum CO₂ conversion for the nickel-based catalysts were 25°C lower in the solar-driven process compared to conventional thermocatalytic process. Meanwhile, the apparent activation energy of the solar-driven reaction is 25% lower than that of the thermocatalytic reaction. Moreover, *in-situ* diffuse reflectance infrared Fourier transform spectroscopy (DRIFTS) experiments were performed to gain an in-depth insight into the enhancement mechanisms of light in the solar-driven process. This study emphasizes the merits of utilizing concentrated solar energy for driving chemical reactions, revealing the promotion of the reaction by light and offering new insights into the reaction mechanism of solar-driven CO₂ methanation over Ni-based catalysts.

Keywords: solar fuel, CO₂ methanation, concentrated solar, mechanism

NONMENCLATURE

Abbreviations	
XRD	X-ray diffraction
SEM	Scan electron microscopy
EDS	Energy dispersive X-ray spectroscopy
BET	Brunauer-Emmett-Teller
UV-Vis DRS	UV-Vis diffuse reflectance spectra
DRIFTS	Diffuse reflectance infrared Fourier transform spectroscopy
Symbols	
X_{CO2}	*Conversion rate of CO₂*
S_{CH4}	*Selectivity of CH₄*
n_{in}	*The amount of feeding gas*
n_{out}	*The amount of produced gas*
GHSV	*Gas hourly space velocity*

1. INTRODUCTION

The emissions of carbon dioxide (CO₂) have emerged as a critical factor in the global climate change challenge, prompting the exploration of innovative strategies to convert CO₂ into valuable fuels and chemicals. CO₂ methanation which know as Sabatier reaction holds promise as a viable approach for recycling and utilizing CO₂, along with the storage and transportation of hydrogen. The CO₂ methanation reaction ($CO_2 + 4H_2 \rightarrow CH_4 + 2H_2O$ $\Delta H_{298K} = -165$ kJ/mol) is a highly exothermic reaction that is thermodynamically favorable but kinetically sluggish at low temperatures. Hence, the use of catalysts and external heat input are usually required to overcome the kinetic limitations imposed by the chemically inert CO₂ molecules.[1] Generally, the industrial Sabatier process is energy intensive, which required high temperature and pressure, and typically

powered by fossil fuels, leading to the extra CO_2 emissions. Renewable energy sources, such as solar and wind power, have taken center stage as transformative solutions for both mitigating climate change and securing sustainable energy supplies. The integration of these renewable energy sources into CO_2 reduction processes shows potential.[2]

In 2014, Ye et al. pioneered the concept of utilizing concentrated solar energy for CO_2 methanation (that is, photothermal catalytic CO_2 methanation).[3] An impressive CH_4 yield of mmol/g/h was achieved using group VIII metal nano-catalysts, which is several orders of magnitude higher than that of conventional photocatalytic processes. Moreover, the photothermal catalytic method offers more favorable reaction conditions and superior performance compared to the thermocatalytic process. It paves the way for harnessing abundant solar energy to effectively mitigate CO_2 emissions.

The majority of research efforts have been dedicated to the development of materials featuring remarkable photothermal conversion properties. Typically, these materials combine active nanometallic substances such as Ru, Au, Ag, and Cu, known for their localized surface plasmon resonance (LSPR) effects, with semiconductors.[4] This approach yields catalysts that exhibit both photocatalytic and thermocatalytic activities. Zou et al. successfully developed an efficient photothermal catalyst denoted as $Ru@Ni_2V_2O_7$, exhibiting broad light-absorption capabilities. The catalyst demonstrated exceptional performance, achieving a CO_2 conversion efficiency of 93.5% and nearly unity CH_4 selectivity under full-spectrum light irradiation.[5] Furthermore, the as-prepared catalyst outperformed both pure $Ni_2V_2O_7$ and $Ru@SiO_2$ catalysts. This superiority was attributed to the unique properties of $Ru@Ni_2V_2O_7$, where Ru nanoparticles served as nano-heaters, and $Ni_2V_2O_7$ generated charge carriers upon light irradiation, facilitating CO_2 reduction via the photocatalytic pathway. The synergistic effect between photocatalysis and photothermal catalysis contributed to the heightened reactivity. However, the utilization of noble metals poses limitations on the scale-up application.

The use of earth abundant transition metals such as Ni, Fe, Co have been considered as the suitable candidates. Among them, Ni has been widely investigated as active component in thermal catalysis CO_2 methanation due to its low price and better catalytic activity.[6] Moreover, Ni also exhibits LSPR effect and can serve as a plasmonic promoter to enhance catalytic performance under light irradiation. Ni-based catalysts, such as Ni/TiO_2,[7] Ni/Al_2O_3, and $Ni/BaTiO_3$,[8] have been developed and widely employed in photothermal CO_2 reduction processes. However, the impact of light on the reaction process remains uncertain and requires further characterization through in-situ approaches.[4]

In this work, we fabricated Ni/Al_2O_3 photothermal catalysts via wet impregnation methods, and the performance of CO_2 methanation was investigated under concentrated full-spectrum light irradiation. The enhancement mechanisms of light in the solar-driven process were demonstrated by activation energy measurement and in-situ diffuse reflectance infrared Fourier transform spectroscopy (DRIFTS) experiments.

2. EXPERIMENTAL

2.1 Synthesis of Ni/Al₂O₃ catalysts

Commercial γ-Al_2O_3 catalysts loaded with varying mass fractions of Ni were synthesized using a wet impregnation method. The detailed procedure was as follows: A specific concentration of $Ni(NO)_3 \cdot 6H_2O$ aqueous solution was prepared, and 5 g of γ-Al_2O_3 was immersed in the solution. The mixture was thoroughly blended and subjected to ultrasonication for 1 hour until a uniformly dispersed solution was achieved. The resulting solution was then dried at 130 °C in an oven overnight. The obtained solid powder was finely ground and subsequently calcined in a muffle furnace at 350 °C for 2 hours, yielding NiO/Al_2O_3 material. Finally, the aforementioned materials were introduced into a tube furnace and heated to 550 ℃ over a period of 2 hours at a rate of 10 °C/ min under a 10% vol H_2/Ar atmosphere, leading to the formation of black Ni/Al_2O_3 materials. By employing the aforementioned procedure, Ni/Al_2O_3 materials loaded with Ni concentrations of 5 wt%, 10 wt%, 15 wt%, and 20 wt% were successfully synthesized.

2.2 Characterization

The morphology of the catalysts was investigated by Scanning electron microscopy (SEM) using a Regulus 8100 microscope. The composition of the synthetized catalyst was studied by energy dispersive X-ray spectroscopy (EDX, Oxford Inca Energy). X-ray diffraction (XRD) patterns were conducted on a Rigaku SmartLab 9kW diffractionmeter with Cu kα radiation (40 kV, 40 mA) with a scanning range from 30° to 80°. UV-Vis diffuse reflectance spectra (UV-Vis DRS) were recorded on a Agilent Carry 7000 UV-Vis spectrometer in the absorption mode ranging from 250 nm-2500 nm. N_2 adsorption-desorption analysis was carried out using a

Micromeritics ASAP 2020 plus instrument after degassing the materials for 12h at 100 ℃, the Brunauer-Emmett-Teller (BET) method was used to determine the surface area of the samples.

2.3 Catalytic performance tests

The experimental system consists of a mass flow meter, thermocouples, quartz glass tubes, an Agilent Mirco 490 model gas chromatograph, a 300W Xenon lamp and a heating furnace. As shown in Fig. 1. The system allows for experimental studies of photothermal-driven and thermal-driven CO_2 methanation.
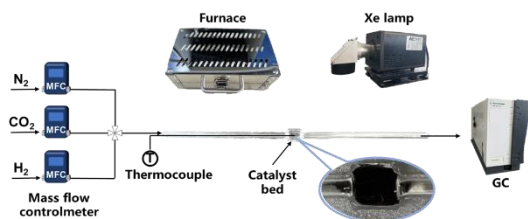
Fig. 1 Schematic diagram of system.

The CO_2 methanation performance of the as-prepared catalysts was assessed as follows: 200 mg of samples were weighed and loaded into the reaction section to ensure a compact fill. Prior to initiating the reaction, a N_2 flow at a rate of 30 mL/min was introduced for purging. Subsequently, a Xenon lamp was opened to illuminate the reaction bed area. Upon reaching a temperature of 250 °C, the inlet gas mixture was adjusted to 5 mL/min of N_2, 5 mL/min of CO_2, and 20 mL/min of H_2 for an additional 5 minutes. Once the temperature stabilized, the outlet gas from the reactor was collected and analyzed every 5 minutes, and the performance was examined across the temperature range of 250-450 °C, with increments of 25 °C as each working condition point. The procedure for the thermal reaction conditions was similar to that of the photothermal conditions. A heating furnace was employed to provide the necessary heat for the reaction.

To ensure the accuracy of the activation energy test and mitigate the influence of heat and mass transfer, the apparent activation energies of the photothermal-driven and thermal-driven processes were evaluated at a gas hourly space velocity of 37500 mL/g/h (25 mL/min of N_2, 25 mL/min of CO_2, and 100 mL/min of H_2). And the CO_2 conversion rate was controlling to remain below 20%. The apparent activation energies were determined in the temperature range of 250-270 ℃, with intervals of 5 ℃ each.

The conversion of CO_2 (X_{CO2}) and selectivity of CH_4 (S_{CH4}) were calculated using the following equations, respectively:

$$X_{CO2} = 100\% * \frac{(n_{CO2})_{in} - (n_{CO2})_{out}}{(n_{CO2})_{in}} \qquad (1)$$

$$S_{CH4} = 100\% * \frac{(n_{CH4})_{out}}{(n_{CH4})_{out} + (n_{CO})_{out}} \qquad (2)$$

2.4 In-situ DRIFTS experiments

In-situ DRIFTS experiments were performed in a Bruker INVENIO S spectrometer equipped with a MCT detector chilled in liquid nitrogen. Before measurement, the catalysts were pre-treated in situ at 350 °C for 1 h under pure H_2 atmosphere. The reduced samples were cooled to the room temperature under high purity Ar flow, and then scanned to get a background spectrum at 25, 250, 300, 350, 400 °C. Subsequently, the inlet gas was switched to a gas mixture consisting of 1% vol CO_2/ Ar for CO_2 adsorption. The temperature was raised from room temperature to 450 °C.

3. RESULT AND DISSCUSSION

3.1 Characterization

The crystal structures of the samples were analyzed by XRD, as shown in Fig. 2. The XRD patterns showed characteristic diffraction peaks of γ-Al_2O_3 and Ni, which correspond well to the standard diffraction cards PDF#50-0741 and PDF#04-0850, respectively. The diffraction peaks at 44.51°, 51.85° and 76.37° were corresponded to the Ni (111), Ni (200) and Ni (220) facets respectively, indicating that Ni species were existed predominantly in the Ni^0 form. It can be found that the intensity of the characteristic peaks corresponding to Ni increased gradually with the escalating Ni loading. In addition, the appearance of other characteristic peaks was not found, indicating that the Ni loading did not change the crystalline phase of Al_2O_3.[7]
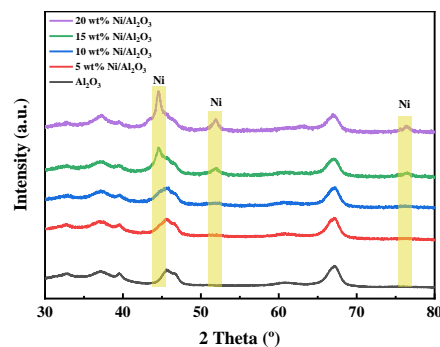

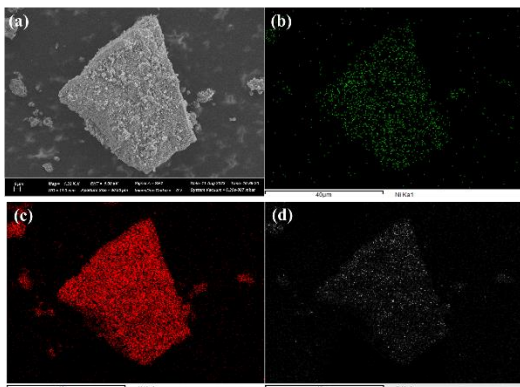Fig. 2 XRD patterns of Ni/Al_2O_3 catalysts

Fig. 3 (a) SEM image and (b)(c)(d) EDX mapping results of of 15 wt% Ni/Al$_2$O$_3$

The strength of light absorption capacity implies whether the material can efficiently harness solar energy. The samples with different mass fractions of Ni loading showed excellent light absorption properties in the UV, visible and IR regions, which is a typical feature of group VIII nanometallic particles.[9] In addition, the light absorption of the samples gradually became stronger with the increase of Ni loading (Fig. 4).
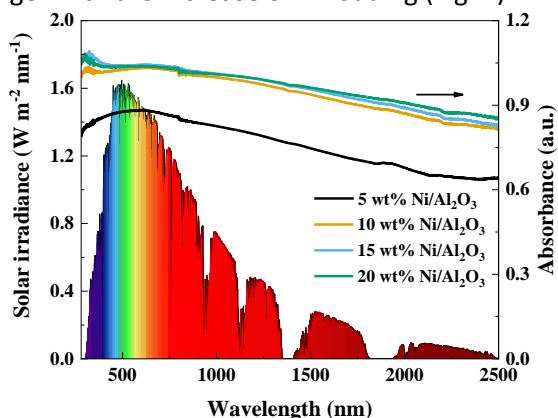

Fig. 4 UV-Vis-IR absorption spectra of Ni/Al$_2$O$_3$ catalysts

Fig. 5 demonstrated the N$_2$ adsorption-desorption isotherm curves recorded at -196 °C for different samples, and the BET specific surface areas and pore sizes of different samples calculated from this curve have been listed in Table 1. It can be found that the specific surface area and pore size of the samples gradually become smaller with the increase of Ni loading, which may be due to the strong interaction between Ni nanoparticles and γ-Al$_2$O$_3$ supports, and the Ni nanoparticles blocked some of the mesopores in the samples after loading.
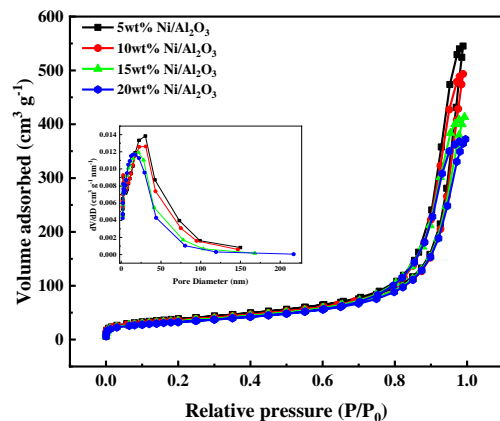

Fig. 5 N$_2$ adsorption-desorption isotherms of Ni/Al$_2$O$_3$ catalysts, the inset is the pore size distribution curves.

Table 1 The results of the characterization of catalysts by N$_2$ adsorption.

Samples	BET surface area (m^2/g)	Pore size (nm)
5 wt% Ni/Al$_2$O$_3$	134.284	25.1185
10 wt% Ni/Al$_2$O$_3$	124.554	24.2945
15 wt% Ni/Al$_2$O$_3$	119.717	21.0867
20 wt% Ni/Al$_2$O$_3$	114.409	19.7569

3.2 Photothermal CO$_2$ methanation tests

The photothermal-driven performances were better than the thermal-driven one before 350 ℃ and exhibited higher CH$_4$ selectivity, which suggested that the concentrated light promoted the conversion of CO$_2$. The highest CO$_2$ conversion was achieved ~86.7% (380 mmol/g$_{Ni}$/h) over 15 wt% Ni/Al$_2$O$_3$ at 350 °C under photothermal-driven condition. As the reaction temperature increased, the difference between the two gradually became smaller, which was attributed to the fact that the reaction kinetics were improved at higher temperatures, and the promotion effect of light was gradually weakened. In addition, when reach the highest CO$_2$ conversion rate, the photothermal-driven processes were reduced by 25 °C compared with the thermal-driven processes. Therefore, the solar-driven process has the potential to reduce the reaction temperature.
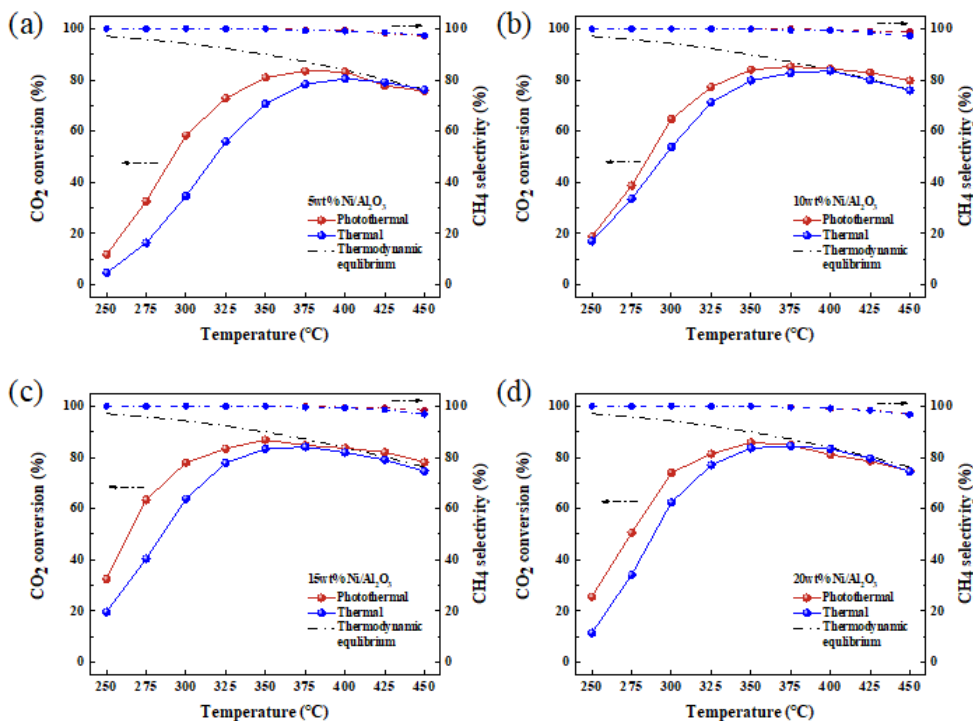
Fig. 6 CO₂ methanation performance under photothermal-driven and thermal-driven conditions at different temperatures over (a) 5wt% Ni/Al₂O₃, (b) 10wt% Ni/Al₂O₃, (c) 15wt% Ni/Al₂O₃ and (d) 20wt% Ni/Al₂O₃

In order to reveal the reason for the difference in reactivity between photothermal-driven and thermal-driven processes, the apparent activation energies of the two were tested and the results of the fitted curves are shown in Fig. 7, with the coefficients of determination, R^2, both of which were 0.99. It can be found that the apparent activation energy of the photothermal process (74.16 KJ/mol) was reduced by about 25% compared to that of the thermal process (92.7 KJ/mol), and the lower activation energy suggested that the CO₂ molecules were more likely to activate under photothermal-driven process and therefore led to higher reactivity.
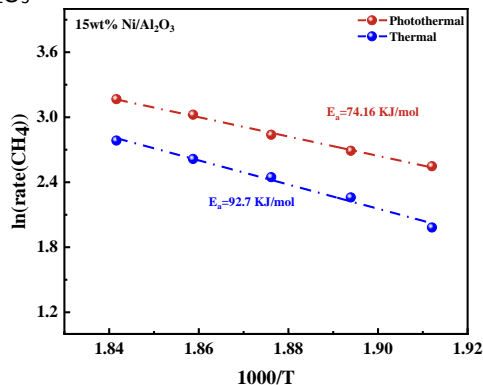

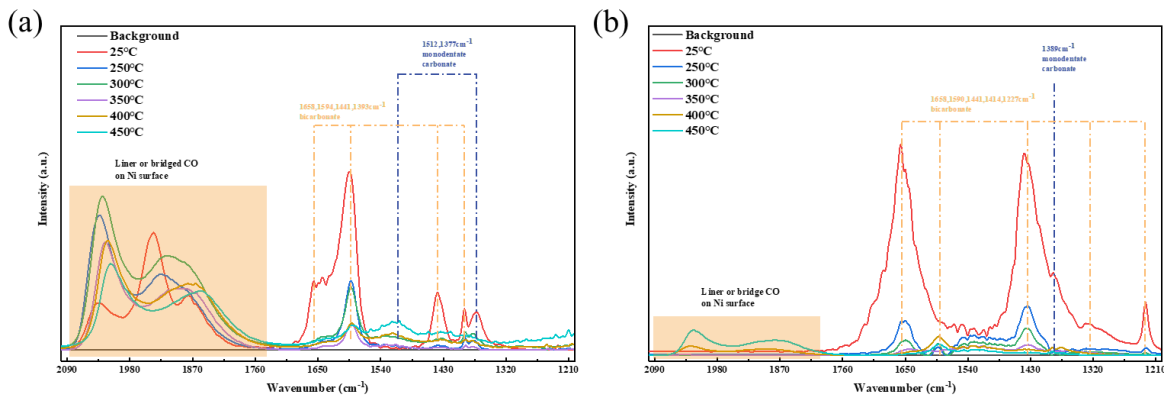Fig. 7 Arrhenius plot of photothermal and thermal-driven process on 15wt% Ni/Al₂O₃.

Fig. 8 In situ DFTIR spectra of CO₂ adsorbed on 15wt% Ni/Al₂O₃ catalysts at different temperatures during (a) photothermal (b) thermal process

5

3.3 In-situ DRIFTS experiments

In-situ diffuse reflectance infrared spectroscopy (DRIFTS) experiments were carried out to further reveal the mechanism of light action in the CO_2 methanation reaction process from a microscopic point of view. The adsorption characteristics of CO_2 on the surface of the material at different temperatures under photothermal-driven and thermal-driven processed were explored, and the results were shown in Fig. 8. It can be found that the adsorption characteristics of CO_2 showed obvious differences. According to the literature, the characteristic peaks in the range of 1800-2100 cm^{-1} can be categorized as bridge *CO (1882, 1840, 1935 cm^{-1}) or line *CO (2000, 2038 cm^{-1}) adsorbed on Ni sites, and the characteristic peaks at 1658, 1590, 1441, 1414, 1393, and 1227 cm^{-1} correspond to adsorbed bicarbonate (*HCO_3^-) on the surface of the material, whereas the peaks at 1512, 1389, and 1377 cm^{-1} correspond to adsorbed monodentate carbonate (*m-CO_3^{2-}). Under photothermal condition, CO_2 was mainly adsorbed on the surface in the form of *CO, *m-CO_3^{2-} and *HCO_3^-, as shown in Fig. 8(a). With the increase of temperature, the intensity of the peaks of *CO gradually increased while the intensity of the peaks of *m-CO_3^{2-} and *HCO_3^- gradually decreased, indicating that *m-CO_3^{2-} and *HCO_3^- were converted to *CO.[10][11]

As shown in Fig. 8(b), CO_2 was mainly adsorbed on the surface in the form of *m-CO_3^{2-} and *HCO_3^- under thermal-driven condition. With the increase of reaction temperature, the intensity of the peaks of *m-CO_3^{2-} and *HCO_3^- decreased gradually, and the peaks of bridged *CO and linear *CO appeared around 400 °C, indicating that part of the carbonate was converted to *CO. The results indicated that it was more difficult to dissociate CO_2 and adsorb it to the Ni site as a *CO species under thermal-driven condition, which is also consistent with previous studies.[12] Number of studies have shown that the activation of CO_2 to *CO is the decisive step for CO_2 methanation, and linear *CO is the key intermediate for further conversion to CH_4, so the subsequent step of methanation is more likely to occur under photothermal condition.[12][13] The above experimental phenomena indicated that CO_2 can be more easily activated, dissociated and adsorbed as *CO on the active sites under the effect of concentrated light. Therefore, light boosted the adsorption of CO_2 on the surface of the sample.

4. CONCLUSIONS

In this paper, Ni/Al_2O_3 catalysts with excellent photothermal conversion characteristics were synthesized, and CO_2 methanation experiments were carried out under photothermal-driven and thermal-driven conditions. The experimental results show that the photothermal-driven process has higher catalytic activity compared with the thermal-driven process, and the temperature was reduced by about 25 °C when the maximum CO_2 conversion was reached. The apparent activation energy test showed that concentrated light effectively reduced the activation energy required for the reaction and could activate CO_2 molecules more easily. At the microscopic level, the results of in-situ DRIFTS experiments showed that concentrated light improved the adsorption and dissociation of CO_2 on the material surface. Our provides new insights into the mechanism of light action in the process of photothermal CO_2 methanation.

DECLARATION OF INTEREST STATEMENT
The authors declare that they have no known competing financial interests or personal relationships that could have appeared to influence the work reported in this paper. All authors read and approved the final manuscript.

REFERENCE
[1] L. Truong-Phuoc, C. Duong-Viet, G. Tuci, A. Rossin, J. Nhut, W. Baaziz, O. Ersen, M. Arab, A. Jourdan, G. Giambastiani, C. Pham-Huu, Graphite Felt-Sandwiched Ni/SiC Catalysts for the Induction Versus Joule-Heated Sabatier Reaction: Assessing the Catalyst Temperature at the Nanoscale, ACS Sustainable Chem. Eng. 2022, 10, 622–632.
[2] F. Zhang, Y. Li, M. Qi, Y. Yamada, M. Anpo, Z. Tang, Y. Xu, Photothermal catalytic CO2 reduction over nanomaterials, Chem Catal. 2021, 1, 1–26.
[3] Meng X, Wang T, Li L, S. Ouyang, P. Li, H. Hu, T. Kako, H. Iwai, A. Tanaka, J. Ye, Photothermal Conversion of CO2 into CH4 with H2 over Group VIII Nanocatalysts: An Alternative Approach for Solar Fuel Production, Angew. Chem. Int. Ed. 2014, 53, 11478 –11482.
[4] Zhou-jun Wang, Hui Song, Huimin Liu, Jinhua Ye, Coupling of Solar Energy and Thermal Energy for

Carbon Dioxide Reduction: Status and Prospects, Angew. Chem. Int. Ed. 2020, 59, 8016-8035.

[5] Y. Chen, Y. Zhang, G. Fan, L. Song, G. Jia, H. Huang, S. Ouyang, J. Ye, Z. Li, Z. Zou, Cooperative catalysis coupling photo-/photothermal effect to drive Sabatier reaction with unprecedented conversion and selectivity, Joule, 2021, 5, 3235–3251.

[6] I. S. Khan, D. Mateo, G. Shterk, T. Shoinkhorova, D. Poloneeva, L. Garzn-Tovar, J. Gascon, An Efficient Metal–Organic Framework-Derived Nickel Catalyst for the Light Driven Methanation of CO2, Angew. Chem. Int. Ed. 2021, 60, 26476–26482.

[7] Y. Li, Z. Rao, Z. Liu, J. Zeng, W. Bao, Z. Wang, J. Li, F. Yu, B. Dai, Y. Zhou, Photo-Assisted CO/CO2 Methanation over Ni/TiO2 Catalyst: Experiment and Density Functional Theory Calculation, ChemCatChem, 2022, 14, e202200182.

[8] D. Mateo, N. Morlanes, P. Maity, G. Shterk, O. F. Mohammed, J. Gascon, Efficient Visible-Light Driven Photothermal Conversion of CO2 to Methane by Nickel Nanoparticles Supported on Barium Titanate, Adv. Funct. Mater. 2020, 2008244.

[9] A. Cárdenas-Arenasa, A. Quindimilb, A. Davó-Quiñonero, E. Bailón-Garcíaa, D. Lozano-Castellóa, U. De-La-Torreb, B. Pereda-Ayob, J.A. González-Marcosb, J.R. González-Velascob, A. Bueno-López, Isotopic and in situ DRIFTS study of the CO2 methanation mechanism using Ni/CeO2 and Ni/Al2O3 catalysts[J]. Appl. Catal. B, 2020, 265, 118538.

[10] Y. Xie, J. C., X. Wu, J. Wen, R. Zhao, Z. Li, G. Tian, Q. Zhang, P. Ning, J. Hao, Frustrated Lewis Pairs Boosting Low-Temperature CO2 Methanation Performance over Ni/CeO2 Nano-catalysts, ACS Catal., 2022, 23, 10587-10602.

[11] X. Xu, L. Liu, Y. Tong, J. Wen, R. Zhao, Z. Li, G. Tian, Q. Zhang, P. Ning, J. Hao, Facile Cr3+-Doping Strategy Dramatically Promoting Ru/CeO2 for Low-Temperature CO2 Methanation: Unraveling the Roles of Surface Oxygen Vacancies and Hydroxyl Groups, ACS Catal., 2021, 11, 5762–5775.

[12] Y. Guo, S. Mei, K. Yuan, D. Wang, H. Liu, C. Yan, Y. Zhang, Low-Temperature CO2 Methanation over CeO2‑Supported Ru Single Atoms, Nanoclusters, and Nanoparticles Competitively Tuned by Strong Metal–Support Interactions and H‑Spillover Effect, ACS Catal., 2018, 8, 6203–6215.

[13] G. Wang, C. He, R. Huang, J. Mao, D. Wang, Y. Li, Photoinduction of Cu Single Atoms Decorated on UiO-66-NH2 for Enhanced Photocatalytic Reduction of CO2 to Liquid Fuels, J. Am. Chem. Soc. 2020, 142, 19339-19345.